THE STRUCTURE OF EXTENSIVE AIR SHOWERS AT SEA LEVEL

A. T. ABROSIMOV, N. N. GORIUNOV, V. A. DMITRIEV, V. I. SOLOV' EVA, V. A. KHRENOV, and G. G. KHRISTIANSEN

P. N. Lebedev Physics Institute, Academy of Sciences, U.S.S.R. and Moscow State University

Submitted to JETP editor December 3, 1957

J. Exptl. Theoret. Phys. (U.S.S.R.) **34**, 1077-1089 (May, 1958)

The lateral distribution of electrons and of nuclear-active and nuclear-passive particles in extensive air showers containing from 4×10^4 to 4×10^5 particles at sea level was studied by means of correlated hodoscopes. The experimental data indicate that cascades of high-energy nuclear-active particles, which determine the development of extensive air showers, are present in the showers in the lower layers of the atmosphere. The energy carried by a cascade is concentrated in a small region with a radius of the order of a few meters around the shower axis.

INTRODUCTION

THE study of the nucleo-cascade process which manifests itself as an extensive air shower requires detailed information concerning the structure of the shower at different heights in the atmosphere. None of the several recent investigations[1-6] of the lateral distributions of the various shower components has been sufficiently thorough. In the present work we endeavored to obtain as complete and accurate quantitative information as possible regarding the lateral distribution of electrons, penetrating nuclear-interacting or "nuclear-active" (n.a.) particles, and "nuclear-passive" (n.p.) particles at sea level. This was a continuation and expansion of the work reported in Ref. 6. The measurements were performed at Moscow from April to June of 1954.

DESCRIPTION OF APPARATUS

We used the well-known method of correlated hodoscopes, described in Ref. 7. The charged-particle distribution was determined by more than 2000 Geiger-Müller counters combined in hodoscope groups that were placed in the plane of observation. Most of these groups (1536 counters) were used to measure the density of all charged particles. The remaining 540 counters detected penetrating n.p. and n.a. particles. Figure 1 shows the general arrangement of the apparatus.

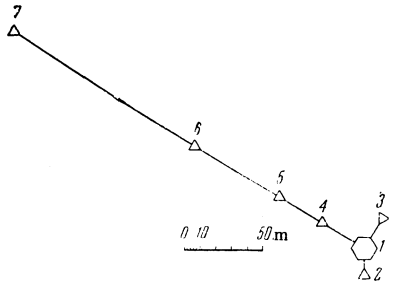

FIG. 1. General arrangement of the apparatus.

The geometry of the apparatus differs from that of Ref. 6 by the presence of the additional hodoscopic stations 5, 6, and 7 located 60, 120 and 250 m, respectively, from the center of station 1.

TABLE I

Number of point	Number of counters: In charged-particle density indicators	Number of counters: In penetrating particle detectors
1	1128	216
2	72	0
3	72	72
4	72	72
5	36	36
6	54	54
7	90	90
Total	1536	540

Table I gives the numbers of counters at stations 1 to 7. The detectors of penetrating particles at stations 1, 3, and 4 were similar to those in Ref. 6, except for the fact that the lead absorber placed above them was increased in thickness from 8 to 13 cm, while the lead shielding at the sides and ends was increased from 10 to 15 cm. Figure 2 is a cross section of the detectors at stations 5, 6, and 7.

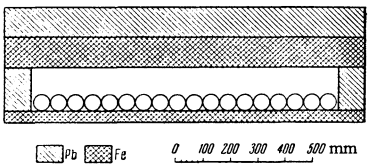

FIG. 2 Detector of penetrating particles at stations 5, 6, and 7.

The hodoscopic arrangement employed in the present work was triggered as described in Ref. 6 by coincidences of six counter groups each of 0.132 m^2 area. The geometry and coincidence arrangement made it possible to study the lateral distributions of all charged particles and n.p. particles 2 to 250 m from the shower axis and of n.a. particles 2 to 30 m from the axis. The total number of particles varied from 10^4 to 10^6 in the showers studied.

In the present work we used GK-6 Korablev hodoscopes at all stations except 7. Because of the time lag of the gaseous discharge in the nonfilamentary thyratrons of the GK hodoscopes, special attention was paid to bringing about agreement between the lag of the master pulse (resulting from the inclination of the shower axis and passage along a high-frequency cable) and the resolving time of each individual hodoscope unit. The latter was measured by the method described in Ref. 8. For units with 6×55 cm^2 counters the average resolving time was 12 microseconds; for 3.3×30 cm^2 counters the resolving time was 8 microseconds and for 2×12 cm^2 counters it was 5 microseconds. With this resolving time, each master pulse was accompanied by not more than a single chance discharge of a counter in the entire hodoscopic system $1-6$. The number of counters triggered legitimately at each of stations $1-6$ considerably exceeded the number due to chance.

With the given system of shower selection the particle density at station 7 is so small that the resolving time must be made as small as possible. Therefore the hodoscope units at station 7 included electron tubes with delay lines and had a resolving time of 2.5 microseconds. This permitted us to study showers at distances of 1 to 250 m from the axis with a minimum of $\sim 10^4$ particles.

METHODS AND RESULTS

The apparatus which has been described furnished a quite detailed picture of the charged particle density distribution near the axis of each recorded shower. This enabled us to determine the required individual characteristics of the shower, which are the position of its axis and the number of shower particles.

In a considerable number of instances the axes of recorded showers passed close to the center of station 1 and the hodoscope groups of counters obtained a good determination of the particle density distribution. In these instances the location of the shower axis was determined without any special assumption regarding the lateral distribution of the shower particles except that of circular symmetry around the axis.

The position of the axis was determined as follows. As the zeroth approximation, the axis was located at the middle of the region of maximum particle density. This region is easily found if the hodoscopes provide a good determination of particle density. For the next approximation we considered the hodoscope groups forming a symmetrical configuration with respect to the middle of the region that had been obtained. Because of the uniform arrangement of hodoscope groups within station 1, a considerable number of these groups entered into this configuration. The "center of gravity" of the region determined in this way was obtained from the formula

$$X_0 = \sum x_i \rho_i / \sum \rho_i, \quad Y_0 = \sum y_i \rho_i / \sum \rho_i,$$

where x_i and y_i are the coordinates of the i-th hodoscope group and ρ_i is the shower particle density above this group. The point X_0, Y_0 is near the shower axis as the "center of gravity" of the entire shower.

For the second approximation we considered the hodoscope groups forming a symmetrical configuration around X_0, Y_0 and determined their center of gravity. In practice the second approximation is unnecessary since the inaccuracy in the determination of X_0, Y_0 is usually much greater than the difference between the first and second approximations.

When the axis passed through the edge or outside of the station its position was determined by making use of the lateral distribution function of shower particles. (This distribution had already been obtained for showers whose axes were located by the method described above.) In such cases we used the fact that the shower axis had to lie on a straight line drawn through the "center of gravity" of the entire hodoscopic station 1 and through its center of symmetry.* We note that when the shower axis passed outside of station 1 but not more distant than stations 2, 3 and 4 its location was also determined, but less accurately. This permitted a considerable increase in the number of showers selected for determination of the particle density at large distances from the axis (stations 5, 6 and 7), where the above-mentioned reduced accuracy evidently played no part.

The average error in locating the axis was 1.5 m when the axis passed within station 1, and 3 m when it passed outside of station 1. When the axis passed within station 1, its rms deviation from this error did not exceed 1 m.

*The hodoscope groups were arranged symmetrically with respect to the center of station 1.

The second shower characteristic, the total number N of the particles, was determined after locating the axis. As a measure of the total number of particles we used the number of particles in the central region of the shower, which was determined directly from the data as $\alpha N = \sum_i \bar{\rho}_i 2\pi r_i \Delta r_i$. Here $\bar{\rho}_i$ is the experimentally observed particle density at distance r_i from the shower axis. In practice this determination of αN is laborious. Therefore, after determining the lateral particle distribution in the central shower region, we followed a different procedure. If the lateral distribution $\rho(r)$ is of the form $\rho(r) = kNf(r)$ the sum of experimentally observed densities is given by $\Sigma\rho_i = kN\Sigma f(r_i)$. Thus $kN = \Sigma\rho_i / \Sigma f(r_i)$. We note that the denominator is independent of the selected form of the lateral distribution function close to its experimental value. The measure kN of the number of particles was determined with an average accuracy of 15%. The number of particles was determined from kN and k, obtained from the form of the lateral distribution function at both small and large distances from the shower axis.

(a) Lateral Distribution of Electrons, Nuclear-Active, and Nuclear-Passive Particles

From a knowledge of the individual shower characteristics and the particle densities at various distances from the axis, we can plot the lateral particle distribution in a single shower. For this purpose it is useful to divide the entire plane of observation into a number of rings around the intersection, with the axis as a center. Since the shower axis is determined with a certain error there is a definite probability that a given ring will include hodoscope counters from within adjacent rings and that some of the counters of the given ring will be found in other rings. The particle density at distance r from the shower axis is determined from the ratio of the average number of triggered and untriggered counters in a given ring of radius r.

However, the lateral distribution of all particles in a single shower is determined with small accuracy. Also, the lateral distribution of penetrating particles cannot be determined for a single shower because the basic construction of the detectors of such particles does not permit obtaining of the particle density in each instance. It is therefore useful to obtain the lateral distribution averaged over a large number of showers with approximately equal total numbers of particles. This lateral distribution is plotted by calculating the particle densities for groups of showers with numbers of particles from N to $N + \Delta N$ striking at distance r from the indicator. Several different cases are possible.

1. The number m of triggered counters is not small compared with the total number n of counters. The average density ρ can then be obtained as the mathematical expectation from the individual densities normalized to the total particle number $\bar{N}$, which is the average for the group of showers under consideration:

$$\bar{\rho} = \sum_i \rho_i (\rho_i/\Delta\rho_i)^2 (\bar{N}/N_i) \Big/ \sum_i (\rho_i/\Delta\rho_i)^2,$$

where $\rho_i\sigma = \ln[n/(n-m)]$ and σ is the area of a single counter. This case occurs in determining the density of all charged particles at stations 1, 2, 3 and 4.

2. The number of triggered counters is subject to the condition $m \ll n$. Then

$$\rho\sigma = \sum_{m=1}^{n} x_m m/n \Big/ \sum_{m=0}^{n} x_m,$$

where x_m is the number of showers corresponding to the triggering of m counters. This definition of the density applies to the calculation for stations 5, 6 and 7 as well as for 2, 3 and 4 in the case of non-dense showers.

3. In determining the density of n.p. and n.a. particles the hodoscopic groups do not give a detailed representation of the density or number of particles striking the counters in a given shower. A hodoscope gives evidence of either the presence or absence of particles. If C is the total number of showers striking at distance r from the detector, C_c is the number of showers registered in the detector of n.p. particles, $\varphi(\rho)\,d\rho$ is the differential density spectrum of all charged particles which is produced by all of the recorded showers, δ is the fraction of n.p. particles by comparison with all charged particles and S is the detector area, then

$$C_c/C = \int (1 - e^{-\delta\rho S})\,\varphi(\rho)\,d\rho \Big/ \int \varphi(\rho)\,d\rho.$$

The density spectrum $\varphi(\rho)\,d\rho$ can be found if we know the spectrum of the number of recorded showers $W(N)\,dN$ and the lateral distribution of charged particles. When $\delta\rho S \ll 1$ the equation becomes $C_c/C = \delta\bar{\rho}S$. For n.a. particles the same equation can be used but with S replaced by $S(1 - e^{-\mu d})$, where $1/\mu$ is the mean interaction path of n.a. particles* in g/cm^2 and d is the quantity of matter in the detector above the lowest tray

*For Pb $1/\mu$ was taken as 160 g/cm^2, and 105 g/cm^2 for Fe.

of hodoscope counters* in g/cm^2.

The type of penetrating particles in the detector was determined from the pattern of discharged counters. The recorded patterns were divided into the following groups:

1. No counter was discharged.
2. One counter or several counters in a single tray were discharged.
3. A single counter was discharged in each of at least two trays. The discharged counters were in a straight line when one counter in each of three trays was discharged.
4. A single counter was discharged in each of at least two trays, but a second counter was discharged in one of these trays.
5. The pattern is a combination of patterns 3 and 4.
6. Several (≥ 3) counters were discharged in one tray; otherwise a single counter in a tray.
7. At least two counters were discharged in one tray and at least four counters in another tray.
8. The counters were discharged at random, but in one tray at least two and in another tray at least three counters were discharged.

TABLE II

Group	1	2	3	4	5	6	7	8
No. of photographs	509	33	14	7	4	8	16	4

Table II gives the distribution of photographs of one of the multi-tray detectors for $\overline{N} = 5 \times 10^4$ according to the groups listed above. The 33 events of group 2 were distributed as follows: One counter was discharged in 25 events, two counters in seven events and three counters in one event.

In the case of penetrating n.p. particles C_c was given by the showers which discharged a single counter in at least two trays (group 3) and C was given by the sum of C_c and C_0, the number of showers which passed through the detector without discharging a single counter (group 1). The density of n.p. particles at distances ≥ 60 m from the shower axis was determined by single-tray detectors. The density of the nuclear-active component at such distances is negligibly small compared with the density of n.p. particles. The firing of each counter was assumed to represent the passage of a single n.p. particle; it was considered that the passage of 7% of the n.p. particles was accompanied by δ electrons and that in such cases two adjacent counters were discharged in a single-tray detector.

In determining the density of n.a. particles C_c was given by the number of showers whose passage through the detector was observed to be accompanied by the formation of a local shower. The observed pattern of the local shower could belong either to group 7 (criterion I for the selection of n.a. particles) or to one of groups 6, 7, or 8 (criterion II).

To plot the lateral distribution we selected showers in which the total number of particles was of the same order of magnitude. To plot the lateral distribution of n.a. and n.p. particles we selected showers with a total number of particles between 2.5×10^4 and 10×10^4 for one group and between 2.5×10^5 and 10×10^5 for another group of showers. $\rho(r)$ was thus determined for a shower in which the total number of particles $\overline{N}$ was the arithmetical mean of N for all the showers striking at a distance r from the center of the detector. At different distances $\overline{N}$ did not vary by more than 10 to 15%. To plot the lateral distribution function we normalized $\rho(r)$ at all distances r to a single value of $\overline{N}$.

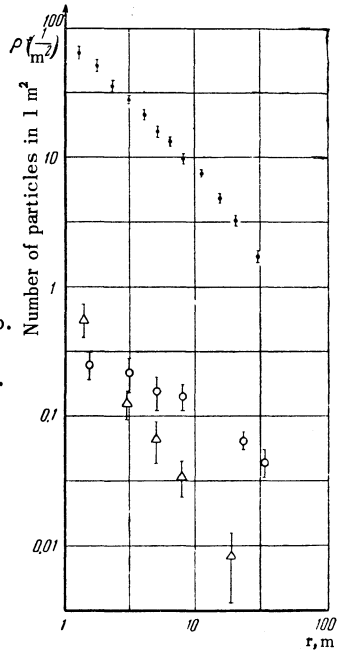

FIG. 3. Lateral distribution: ● – electrons, N = 4.3 × 10^4; △ – n.a. particles, N = 5 × 10^4 (criterion I); ○ – n.p. particles, N = 5 × 10^4; r – distance from shower axis.

The lateral distribution functions are shown in Figs. 3 and 4. Fig. 3 gives the lateral distributions of electrons, n.a. and n.p. particles near the shower axis. Figure 4 gives the lateral distribution of all charged particles and n.p. particles at distances from 2 to 250 m from the shower axis.

Our experimental data on the lateral distribution of all charged particles can be approximated by the function $kNr^{-1}e^{-r/R}$ with $R = (60 \pm 6)$ m

*If we neglect absorption of electron-nucleonic showers in matter we can write

$$C_c/C = \sum_{n=1}^{\infty} \frac{e^{-\delta\rho S}}{n!} (\delta\rho S)^n (1 - e^{-n\mu d}) = 1 - e^{-\delta\rho S (1 - e^{-\mu d})}.$$

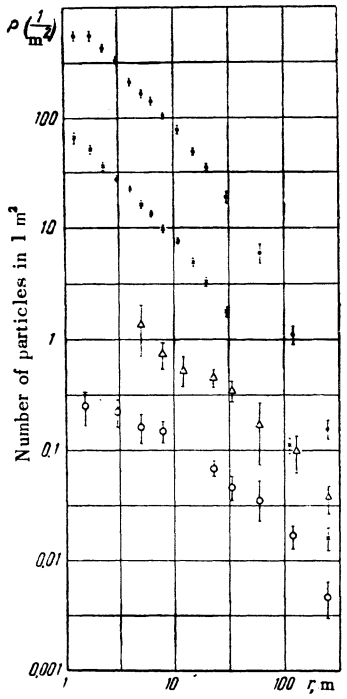

FIG. 4. Lateral distribution of electrons (● – for $N = 4.3 \times 10^4$, × – for $N = 4.3 \times 10^5$) and of n.p. particles (△ – for $N = 5 \times 10^4$, ○ – for $N = 5 \times 10^5$).

for $2 \ll R(n-1)$ and the power law $k_1 N r^{-n}$ for $r \geq R(n-1)$ with $n = 2.6 \pm 0.4$. The coefficients k and k_1 are found by normalizing the lateral distribution function:

$$\int \rho(r)\, 2\pi r dr = N$$

and equating the functions $kNr^{-1}e^{-r/R}$ and $k_1 N r^{-n}$ at the point $r = R(n-1)$. In this way the value $(2.0 \pm 0.3) \times 10^{-3}$ was found for k.

We also note that by using data on the lateral distributions of n.a. and n.p. particles we can determine the minimum numbers of these particles in showers with different $\bar{N}$. These results are given in Table III.

TABLE III

	$\bar{N} = 5 \cdot 10^4$	$\bar{N} = 5 \cdot 10^5$
Number of n.a. particles in a circle of radius R = 22 m	31 ± 6	330 ± 50
Number of n.p. particles in a circle of radius R = 106 m	1860 ± 350	10800 ± 4000

(b) Absolute Number of Showers

Our hodoscopic setup served at the same time to determine the number of recorded extensive air showers with a given number N of particles. From this number, the absolute number of showers with N particles and with axes, striking at an angle $\theta = 0$ with the vertical, per unit area and unit solid angle, can be obtained from the following equation:

$$C(N)\Delta N = \int_0^{\pi/2}\int_0^{2\pi}\int_S F(N, \theta)\, W(N, \theta, \varphi, x, y) \times \cos\theta \sin\theta\, d\theta\, d\varphi\, dx\, dy\, \Delta N.$$

Here $C(N)\Delta N$ is the number of recorded showers with N to $N + \Delta N$ particles and axes striking the region S of the xy plane; $F(N, \theta)$ is the number of showers with N particles and axes inclined at angle θ to the vertical on the xy plane, per unit area in the xy plane, per unit interval of N, and per unit solid angle:

$$F(N, \theta) = F(N, 0)\cos^{\nu}\theta;$$

$$W(N, \theta, \varphi, x, y) = \prod_{i=1}^{6}(1 - e^{-\rho_i \sigma_i})$$

is the probability that the control system will record a shower with N particles, with its axis striking the point x, y at angle θ to the vertical and with the azimuthal angle φ; $\rho_i = Nf[r_i(\theta, \varphi)]$ r_i is the distance from the shower axis to counter group i connected for coincidences in the plane perpendicular to the shower axis.

Station 1 was taken for the region S, since the location of a shower axis passing through this station and the number of shower particles are obtained most accurately. Then r_i is the distance from the shower axis to the center of station 1, which is the location of the counter groups included in the control system.

For a sufficiently steep angular distribution of the axes and sufficiently slow decline of particle density away from the axis $C(N)\Delta N$ can be written as follows:*

$$C(N)\Delta N = \int_0^{\pi/2}\int_0^{2\pi} F(N, 0)\cos^{\nu+1}\sin\theta\, d\theta\, d\varphi \times \int_S W(N, x, y)\, dx\, dy\, \Delta N.$$

For showers with a large number of particles $N \gg 1/\sigma f(r)$

$$\int_S W(N, x, y)\, dx\, dy \approx 1,$$

$$C(N)\Delta N = F(N, 0)(2\pi/\nu + 2) S \Delta N.$$

For showers with smaller N, this integral was calculated numerically.

Table IV gives data on $F(N, 0)$ at sea level assuming that the angular distribution of shower axes is represented by $\cos^2\theta$ with $\nu = 7.5$ (Ref. 9) for showers with different numbers N of particles.

*For the recorded showers, when account is taken of the fact that the recording probability W is dependent on θ and φ, there is not more than a 5% change in $C(N)\Delta N$.

DISCUSSION

The data of the present work, together with an investigation of shower structure at mountain altitudes, permit us to draw certain conclusions regarding the character of the nucleonic cascade.

TABLE IV*

N ± ΔN	F(N, 0) N 1/cm²-sec-sterad
$2.6 \cdot 10^5 \pm 3.4 \cdot 10^4$	$1.43 \cdot 10^{-10} \pm 2.86 \cdot 10^{-11}$
$2.7 \cdot 10^4 \pm 4.0 \cdot 10^3$	$4.1 \cdot 10^{-9} \pm 8.2 \cdot 10^{-10}$

*We here consider only a small fraction of all recorded showers with large N.

These conclusions are derived indirectly, not on the basis of an experimental study of the nucleonic cascade itself, but from analysis of experimental material concerning the different components of an extensive air shower which accompany that process. We also note that these experimental results represent averaged characteristics rather than any single shower.

We shall first consider the general behavior of a shower in the lower layers of the atmosphere. Figure 5 shows the lateral distribution of electrons

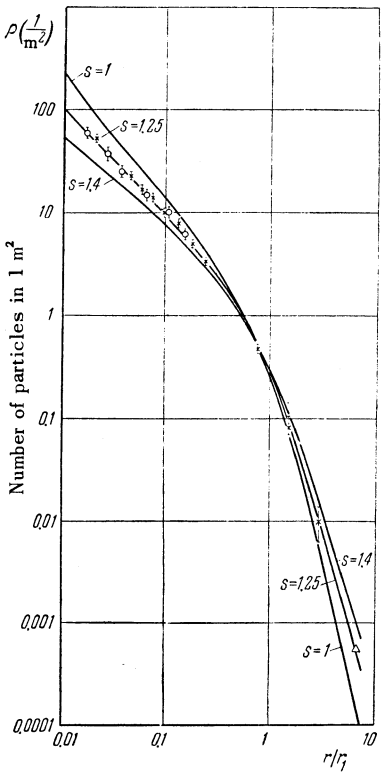

FIG. 5. Lateral distribution of electrons: × – at Moscow with $\bar{N} = 4.3 \times 10^4$, o – at the Pamir mountain site with $\bar{N} = 7 \times 10^4$ and the curves of Nishimura and Kamata for s = 1, 1.25 and 1.4. The observations were normalized with the curve for s = 1.25 to the number of particles in a circle of 250 m radius. r/r_1 is the distance from the shower axis in units of r_1.

in extensive air showers at sea level (from data of the present work) and at a mountain altitude (Ref. 10) in showers with similar total numbers of particles. The unit of length is the Molière parameter $r_1 = E_S x_0/\beta$, where $E_S = 19$ Mev, β is the critical energy for air, and x_0 is the length of one radiation unit in meters at the level of observation. The figure shows that when a quantity proportional to x_0 is taken as the unit of length the lateral distribution of electrons is identical at sea level and at a mountain altitude.

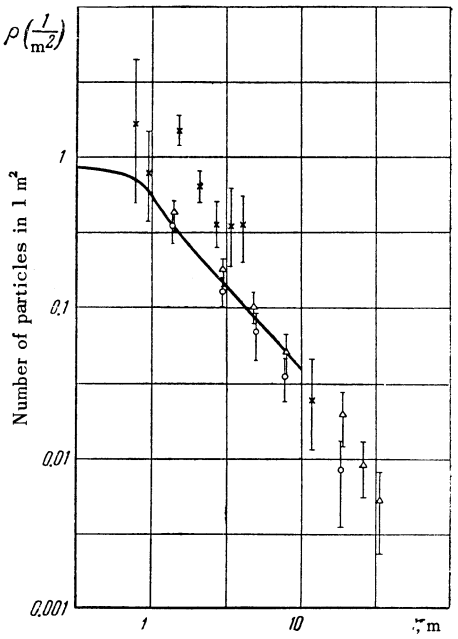

FIG. 6. Lateral distribution of n. a. particles at Moscow for $\bar{N} = 5 \times 10^4$: o – criterion I, Δ – criterion II; × – the same at the Pamir altitude for $\bar{N} = 6.5 \times 10^4$. The solid curve was calculated from Eq. (1) for ρ(r), where r is the shower axis for Moscow.

Figure 6 shows the lateral distribution of n.a. particles in extensive air showers at sea level and a mountain altitude.[11] The distance from the shower axis is measured in units of length which are inversely proportional to the atmospheric pressure at the level of observation. The two distribution functions are seen to have approximately the same shape. We also note that the same data give approximately the same absolute number of n.a. particles at both altitudes in showers with similar N. Finally, Fig. 7 gives the lateral distribution of μ mesons at sea level and a mountain altitude[12] in showers with the same N.

On the basis of the data presented we can state that in the investigated range of distances from the shower axis the μ-meson component is identical in showers at different altitudes. There are two possible explanations of this observed similarity at two altitudes.

1. The observed similarity is associated with the characteristics of the development of a nucleonic cascade in the lower atmospheric layers.

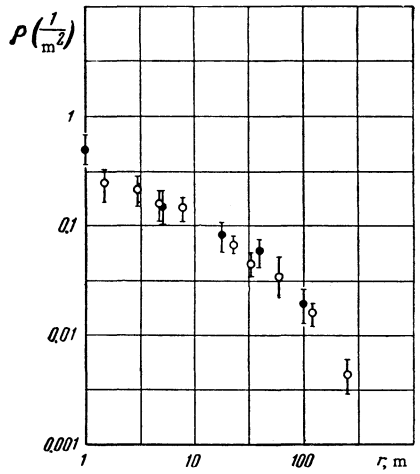

FIG. 7. Lateral distribution of nuclear passive (n.p.) particles: o – at Moscow, $N = 5 \times 10^4$, • – for the Pamir altitude, $\bar{N} = 5 \times 10^4$, r – distance from the shower axis.

2. The similarity results from the fact that showers observed at different altitudes are on the average at the same stage of development.

According to the second explanation the generation of the observed showers must occur not only in high atmospheric layers but also deep in the atmosphere, which is actually possible with a sufficiently small interaction cross section for the primary particles that initiate the showers.

In this connection, let us consider the data on the lateral distribution of μ mesons, which is determined by the angular divergence of the π and K mesons from which the μ mesons originate and also, as was shown in Ref. 13, to a considerable extent by Coulomb scattering. Thus the lateral distribution of μ mesons is very sensitive to the height at which they are generated. In the second explanation of the similarity it is assumed that this height of generation, measured in g/cm^2, is approximately the same for the two altitudes of observation. It would thus follow that the lateral divergence of μ mesons at sea level would be smaller than at mountain altitudes. According to observations (Refs. 14 and 15) the lateral distribution of μ mesons at sea level is characterized by a more slowly diminishing function than at mountain altitudes. We shall therefore dwell in greater detail on the first explanation and shall consider the characteristics of the development of the nucleonic cascade which follow from the results of shower observations.

We now turn to an analysis of data on the electronic component, whose lateral distribution must be determined by Coulomb scattering of electrons and possibly by the lateral distribution of the cores of elementary cascades which results from the angles of emission of π^0 mesons in elementary acts of the nucleonic cascade process. The problem of the lateral distribution of electrons in electron-photon cascades characterized by the shower development parameter s has been solved by Nishimura and Kamata and by Greisen.[16] Figure 5 gives the lateral distribution of electrons and the theoretical curves for different s.

The lateral distribution due to Coulomb scattering is known to be determined by the energy spectrum of the electrons $N(>E) \sim E^{-s}$. From data on the barometric effect and angular distribution of shower axes[16] it follows that $s = 1.2$, since the absorption coefficient of the number of particles in a shower is $\lambda(s) = 1/200$ g/cm^2. Direct measurements of electron energy spectrum in extensive air showers[17] are not in disagreement with this value of s. Figure 5 shows that the theoretical curve of Nishimura, Kamata and Greisen with this value of s furnishes the best agreement with observation.

Agreement of the theoretical and experimental curves over the broad distance interval $0.02 < r/r_1 < 3$ cannot, of course, be fortuitous. It is thus reasonable to conclude that the lateral divergence of individual electron-photon cascade cores does not essentially influence the lateral distribution of electrons. Thus the energy borne by a nucleonic cascade must be well concentrated around the shower axis. The degree of this concentration can be estimated directly. If the divergence of electrons from the shower axis is due only to Coulomb scattering the distribution of the energy of the electron-photon component near the shower axis must be $1/r^2$ * according to cascade theory. If the lateral distribution of electrons with the given energy spectrum is to be essentially that due to Coulomb scattering alone, then the lateral distribution of the energy borne by a nucleonic cascade must be steeper than that borne by the electron-photon component, that is, it must be steeper than $1/r^2$. From the form of the lateral distribution of electrons it is also possible to estimate the energy of n.a. particles which produce electron-photon showers through π^0 mesons. Such an estimate,[18] based on the fact that s is independent of distance from the shower axis, gives $E_{n.a.} \geq 10^{11}$ ev.

Let us now consider our data on the nuclear-active component in the central region of a shower. From the preceding analysis it appears that most of the shower of a nucleonic cascade is concentrated close to the shower axis. An analysis of the lateral distribution of n.a. particles can indicate the effective size of this circumaxial region.

*Observation[17] of the energy distribution of the electron-photon component near the shower axis also agrees with $\sim 1/r^2$.

We have calculated the lateral distribution of n.a. particles using the following assumptions. The flux of high-energy n.a. particles is concentrated in a circle of radius a around the axis of an extensive air shower. Our recorded n.a. particles of relatively low energies are generated by the high-energy n.a. particles isotropically within a certain angle θ in the laboratory system. Neglecting the absorption coefficient of both high-energy and low-energy n.a. particles, the density of n.a. particles with low energies is given by

$$\rho(r) = \int_0^{2\pi}\int_0^{a}\int_{x_{\min}}^{\infty} \frac{x\,dx\,r'\,dr'\,d\varphi}{[r^2 + r'^2 - 2rr'\cos\varphi + x^2]^{3/2}};$$

$$x_{\min} = \frac{\sqrt{r^2 + r'^2 - 2rr'\cos\varphi}}{\tan\theta}, \qquad (1)$$

where x is the height above the altitude of observation, r is the distance from the shower axis to the point of observation, x_{min} is the minimum height beginning with which particles start to strike at the distance r from the axis after being emitted at the angle θ, and the vector $\mathbf{r}'\{r', \varphi\}$ defines the position of high-energy n.a. particles with respect to the shower axis. Integration gives*

$$\rho(r) = \begin{cases} 4Cr\left[E\left(\frac{a}{r}\right) + \left(\frac{a^2}{r^2} - 1\right)K\left(\frac{a}{r}\right)\right]; & \frac{a}{r} < 1 \\ 4CaE\left(\frac{r}{a}\right); & \frac{a}{r} > 1, \end{cases}$$

where C is a constant depending on the angle θ. The function $\rho(r)$ calculated in this way is shown in Fig. 6; comparison with observation shows that a must be $\lesssim 1$ m.

We shall use this result to estimate the energy of n.a. particles in a nucleonic cascade. It is known that the average angle of nuclear scattering cannot be smaller than $\mu_\pi c^2/E$ (as a result of the meson character of nuclear forces). This angular deviation is acquired on the average in one mean free nucleon path. Thus we must have $(\mu c^2/E)X \leq a$, whence†

$$E > 5 \cdot 10^{10}\ \text{ev}.$$

The combined experimental data on the electron-photon and nuclear-active components of extensive air showers at different altitudes lead to the conclusion that in the lower layers of the atmosphere down to sea level the high-energy ($\gtrsim 10^{11}$ ev) n.a. particles which determine the development of the entire shower are concentrated around the shower axis. Thus the nucleonic cascade plays an essential role in shower development within low-lying atmospheric layers. The development of the electron-photon component will then be closely related to the development of the nucleonic cascade. When n.a. cascade particles interact with the nuclei of air atoms a portion of their energy is imparted to π^0 mesons. Photons from the decay of the π^0 mesons give rise to elementary electron-photon cascades. Thus at a depth t of observation the number of electrons is

$$N(t) = \int_{E_0}\int_0^t f(E_0,\ t')\,N(E_0,\ t - t')\,dE_0\,dt',$$

where $f(E_0, t')$ is the number of photons with energy E_0 which result from the decay of π^0 mesons generated at depth t' in the atmosphere and $N(E_0, t-t')$ is the total number of electrons at the level of observation from a photon of energy E_0.

The absorption of the electron component of a shower in the lower atmosphere will be determined to a considerable extent by the form of $f(E_0, t')$. In the limiting case equilibrium is possible between the electron component and the nucleonic cascade.* For this case, assuming that the total energy F(t) imparted to π_0 mesons varies with the depth as $\sim e^{-\mu t}$ and using the theorem of the mean, we have

$$N(t)\beta = \int_{E_0} f(E_0,\ t - t^*)\int_0^t N(E_0,\ t - t')\,\beta\,dt'\,dE_0$$

$$= \int_{E_0} f(E_0,\ t - t^*)\,E_0 dE_0 = F(t - t^*) = F(t)\,e^{\mu t^*},$$

since the essential values of $(t-t')$, much less than t and t*, have a slight logarithmic dependence on E_0. Thus in equilibrium the number of shower particles diminishes according to the same law as the energy of the nucleonic cascade.

Table IV gives the absolute intensity of showers with different N at sea level. At the Pamir altitude Nikol'skii et al. similarly obtained the absolute number of showers with $N \approx 2.6 \times 10^5$ assuming the angular distribution of shower axes to be $\cos^2\theta$ with $\nu = 5.5$ (Ref. 9). Their result was $(1.37 \pm 0.27) \times 10^{-9}$ cm^{-2}-sec^{-1}-sterad^{-1}. From the absolute shower intensities at the two altitudes we can determine the absorption coefficient of showers with a given number of particles and the absorption coefficient of the number of particles in a shower. The latter coefficient was calculated to be $1/\mu = 1/200$ cm^2/g and, as indicated above,

*E(a/r) and K(a/r) are complete elliptic integrals (see Ref. 19).

†G. T. Zatsepin was the first to estimate the energy of n.a. particles from the same considerations; see also Ref. 20.

*Equilibrium between the electron-photon component and the nucleonic cascade was also considered by G. T. Zatsepin and I. L. Rozental' (report at a seminar of the Physics Institute, Academy of Sciences, U.S.S.R.)

can be regarded as the absorption coefficient of the energy borne by the nucleonic cascade in the equilibrium case.

All these observations (identity of the lateral distributions at the two altitudes, approximately identical variations with height of both electrons and nuclear-active particles) can be explained by postulating equilibrium between the electron component and the low-energy nuclear-active component on the one hand, and the energy of the nucleonic cascade of the shower core on the other hand.

In conclusion, we shall estimate the minimum total energy of a nucleonic cascade close to the level of observation assuming that the $\pi^{\pm}$ mesons produced in interactions have only a small probability of decaying to μ mesons. For equilibrium we have

$$N(t)\beta = F(t)\,e^{\mu t^*}.$$

We assume the energy of the nucleonic cascade to be $W(t) = F(t)/\mu$. Hence the energy of a nucleonic cascade which has reached the depth t is

$$W(t) = W_0 e^{-\mu t} = N(t)\beta/\mu e^{\mu t^*}.$$

The magnitude of t^* is evidently close to the mean path of an elementary electron-photon cascade. Thus, taking $t^* = \ln E_0/\beta$, we have

$$W(t) = N(t)\beta/\mu\,(E_0/\beta)^{\mu}.$$

Assuming $E_0 = 10^{10}$, $\beta = 7 \times 10^7$ ev and $\mu = 0.17$, we obtain for $N \approx 10^4$

$$W(t) \approx 10^{12} \text{ ev}.$$

In conclusion, the authors wish to thank N. A. Dobrotin for considerable assistance and interest, and S. N. Vernov and G. T. Zatsepin for discussions of the results. G. V. Bogoslovskii, V. I. Zatsepin, V. Ia. Markov, A. M. Mozhaev, B. V. Subbotin, M. S. Tuliankina, and E. I. Tukish, who assisted with the adjustment of the apparatus and with the measurements, are also entitled to the thanks of the authors.

[1] H. L. Kasnitz and K. Sitte, Phys. Rev. **94**, 977 (1954).

[2] S. R. Haddara and D. Jakeman, Proc. Phys. Soc. (London) **A66**, 549 (1953).

[3] R. E. Heinman, Phys. Rev. **96**, 161 (1954).

[4] G. Fujioka, J. Phys. Soc. Japan **10**, 246 (1955).

[5] Hazen, Williams and Randall, Phys. Rev. **93**, 578 (1954).

[6] Abrosimov, Bedniakov, Zatsepin, Nechin, Solov' eva, Khristiansen, and Chikin, J. Exptl. Theoret. Phys. (U.S.S.R.) **29**, 693 (1955), Soviet Phys. JETP **2**, 357 (1956).

[7] G. T. Zatsepin, Dissertation Phys. Inst., Acad. Sci. U.S.S.R., 1954.

[8] G. B. Khristiansen, Приборы и техника эксперимента (Instruments and Instr. Engg.) **1**, 48 (1958).

[9] H. L. Kraybill, Phys. Rev. **93**, 1362 (1954).

[10] Vavilov, Nikol' skii, and Tukish, Dokl. Akad. Nauk SSSR **93**, 233 (1953).

[11] Batov, Nikol' skii, and Vavilov, Dokl. Akad. Nauk SSSR **111**, 71 (1956), Soviet Phys. "Doklady" **1**, 625 (1957).

[12] Dovzhenko, Nelepo, and Nikol' skii, J. Exptl. Theoret. Phys. (U.S.S.R.) **32**, 463 (1957), Soviet Phys. JETP **5**, 391 (1957).

[13] G. B. Khristiansen, J. Exptl. Theoret. Phys. (U.S.S.R.) **34**, 956 (1958), Soviet Phys. JETP 661 (1958).

[14] Antonov, Vavilov, Zatsepin, Kuruzov, Skvortsov, and Khristiansen, J. Exptl. Theoret. Phys. (U.S.S.R.) **32**, 227 (1957), Soviet Phys. JETP **5**, 172 (1957).

[15] Eidus, Adamovich, Ivanovskaia, Nikolaev, and Tuliankina, J. Exptl. Theoret. Phys. (U.S.S.R.) **22**, 440 (1952).

[16] K. Greisen, Progress in Cosmic Ray Physics, Ed. Wilson, **3** (Amsterdam, 1956).

[17] Ivanovskaia, Kulikov, Rakobol' skaia, and Sarychev, J. Exptl. Theoret. Phys. (U.S.S.R.) **33**, 358 (1957), Soviet Phys. JETP **6**, 276 (1958).

[18] G. B. Khristiansen, Oxford Conference on Extensive Air Showers, 1956.

[19] I. N. Bronshtein and K. A. Semendiaev, Справочник по математике (Mathematics Handbook), 1953.

[20] Iu. N. Vavilov, J. Exptl. Theoret. Phys. (U.S.S.R.) **33**, 179 (1957), Soviet Phys. JETP **6**, 141 (1958).

Translated by I. Emin
226